Waste Management 97 (2019) 71–81

Contents lists available at ScienceDirect

Waste Management

journal homepage: www.elsevier.com/locate/wasman

Recycling of sisal fiber reinforced polypropylene and polylactic acid composites: Thermo-mechanical properties, morphology, and water absorption behavior

Chakaphan Ngaowthong [a,b,c], Martin Borůvka [d], Luboš Běhálek [d], Petr Lenfeld [d], Martin Švec [e], Rapeephun Dangtungee [a], Suchart Siengchin [a,*], Sanjay Mavinkere Rangappa [a], Jyotishkumar Parameswaranpillai [c,*]

[a] Department of Mechanical and Process Engineering, The Sirindhorn International Thai – German Graduate School of Engineering (TGGS), King Mongkut's University of Technology North Bangkok, 1518 Pracharat 1 Road, Bangsue, Bangkok 10800, Thailand
[b] Department of Agricultural Engineering for Industry, Faculty of Industrial Technology and Management, King Mongkut's University of Technology North Bangkok Prachinburi Campus, 29 Moo 6, Tumbon Noenhom, Amphur Muang, Prachinburi 25230, Thailand
[c] Center of Innovation in Design and Engineering for Manufacturing (CoI-DEM), King Mongkut's University of Technology North Bangkok, 1518 Pracharaj 1, Wongsawang Road, Bangsue, Bangkok 10800, Thailand
[d] Department of Engineering Technology, Faculty of Mechanical Engineering, Technical University of Liberec, Studentská 2, 461 17 Liberec 1, Czech Republic
[e] Department of Materials, Faculty of Mechanical Engineering, Technical University of Liberec, Studentská 2, 461 17 Liberec 1, Czech Republic

ARTICLE INFO

Article history:
Received 29 April 2019
Revised 10 July 2019
Accepted 29 July 2019
Available online 3 August 2019

Keywords:
Polypropylene
Polylactic acid
Thermomechanical properties

ABSTRACT

The effect of recycling on the thermo-mechanical and water absorption behavior of polypropylene (PP)/sisal fiber and polylactic acid (PLA)/sisal fiber composites were studied. The PP-based non-biodegradable composites and PLA-based biodegradable composites were recycled for four times. The effect of recycling was determined by examining the morphology, thermo-mechanical properties, and water absorption behavior and the obtained results were compared. The results showed that the incorporation of sisal fibers in the PP and PLA matrix enhances the tensile modulus and percentage crystallinity of the composites. The tensile strength and modulus of the sisal fiber reinforced PP composites were not affected with recycling. Even though the tensile properties of PLA and PLA/sisal fiber reinforced composites are superior to PP and PP/sisal fiber composites, the PLA-based composites show a dramatic decrease in tensile strength and modulus after the first recycling due to the degradation of the polymer. The thermal stability of the PP/sisal fiber composites was not affected by the repeated recycling process. On the other hand, the PLA-based composites with higher sisal fiber content show a bit lower thermal stability after recycling. The PP-based composites show fluctuations in percentage crystallinity with recycling. On the other hand, a remarkable increase in percentage crystallinity for PLA and PLA-based composites was observed with increasing recycling times. Water diffusion study divulges that the diffusion of water into the polymer composites was reduced with recycling, irrespective of the polymer matrix.

1. Introduction

The mass production of plastics begins in 1950 since then the manufacturing of plastics has grown tremendously. Of the 6.3 billion metric tons of plastic waste generated over the years, approximately 9% is recycled of which only 10% of the plastic has been recycled more than one time (Geyer et al., 2017). Therefore, recycling, recovery, and management of synthetic plastics is a cause for concern. Moreover, the cost of making virgin plastics is too high and also deplete natural resources. However, recycling is environmentally friendly, low cost and energy-efficient. It should be pointed out that of the total waste generated, polypropylene (PP) accounts the major share of 23% (Chen et al., 2019). On the other hand, polylactic acid (PLA) is a biodegradable plastic synthesized from plant products and has good strength and modulus and is an alternative to PP, but has poor impact strength (Elsawy et al., 2017). The global production of PLA is roughly 0.2 million tons in 2017. However, no information is available on the percentage of

* Corresponding authors.
E-mail addresses: suchart.s.pe@tggs-bangkok.org (S. Siengchin), jyotishkumarp@gmail.com (J. Parameswaranpillai).

https://doi.org/10.1016/j.wasman.2019.07.038
0956-053X/

global waste of PLA composites. Utilization of agro-waste, especially natural fibers for making polymer composites has been attracted considerable attention in recent years due to the particular interest on environmental protection and to take the full advantage of natural fibers. The advantages of natural fibers over synthetic fibers are utility of agro-waste, low cost, fully biodegradable, renewable, low energy for processing, no release of toxic gases during production or processing of the fibers, lower environmental damage, lightweight, good strength and modulus, dimensional stability, thermal stability, chemical resistance etc. (Das et al., 2010; Abba et al., 2013; Hoang et al., 2010; Cestari et al., 2019). In connection with this, the natural fibers extracted from plants have been used as a reinforcement in polymer matrices to improve the properties of the plastics (Abraham et al., 2012; Thomas et al., 2015; Sanjay et al., 2018; Senthilkumar et al., 2018; Sanjay et al., 2019). It is important to add that the temperature of polymer processing, fiber processing, polymer type, molecular weight, mixing time, mixing temperature etc., may influence the properties of the polymer composites. In recent years, a lot of attention has been drawn with the recycling of composites made from natural fibers and polymer matrices (Bourmaud and Baley, 2007; Cicala et al., 2018; Beltrán et al., 2019). Some studies reported recycling of waste plastics and natural fibers to produce value-added products (Najafi, 2013; Gu and Ozbakkaloglu, 2016; Singh et al., 2017). Chianelli-Junior et al. (2013) discussed the mechanical performance and the possibilities of sisal fibers as a reinforcement for recycled high-density polyethylene (rHDPE). It was observed that there is no change in the tensile and flexural properties of the rHDPE with the addition of sisal fibers. However, the ductility decreases in the presence of sisal fibers. Favaro et al. (2010) prepared rHDPE reinforced with sisal fibers. The authors proved that the chemically modified sisal fibers can improve their compatibility with HDPE. Ibrahim et al. (2017) reported that the inclusion of chemically treated sisal fiber, nanoclay, and maleic anhydride grafted polypropylene (MA-g-PP) in the recycled polypropylene (rPP) nanocomposites enhances the mechanical properties and decreases the water absorption. Srivabut et al. (2018) determined the thermo-mechanical and water absorption behavior of rPP/rubberwood flour composites with different fillers such as nanoclay, talcum, and calcium carbonate. The authors reported that the presence of chemical fillers in PP/rubberwood flour composites improves the mechanical properties, crystallinity, and reduces the water absorption, thus facilitate the development of new engineering materials using recycled wood and PP.

Several authors have studied the recycling of PP and PLA based natural fiber composites. Arzondo et al. (2005) demonstrated the work on long sisal fiber/PP reinforced composites using MA-g-PP as a compatibilizer. This work has shown that the fiber breakage is minimum for the recycled composites, due to the wetting of the polymer layer on the sisal fibers. Dairi et al. (2017) worked on PP/recycled polyethylene terephthalate (r-PET) composite materials filled with wood flour (WF). The results indicated that the MA-g-PP acts as an effective compatibilizer in PP/r-PET/WF composites. Cicala et al. (2017) evaluated the mechanical properties of the PP modified with MA-g-PP, liquid wood, and hemp fibers. Recycling studies showed that the developed polymer composites can sustain at least two recycling without much loss of properties. Laadila et al. (2017) reported enhanced mechanical properties for the recycled biocomposites based on polylactic acid (rPLA) and treated cellulose fibers in comparison with rPLA.

Thus, from the literature, few authors have been reported studies on recycling of natural fibers reinforced PP and PLA composites. However, a systematic study on the effect of recycling of PP/sisal fiber and PLA/sisal fiber composites on the tensile properties, thermal stability, crystallinity, and water absorption has not been reported till date. In this work, the effect of recycling on the tensile properties, morphology, thermogravimetric analysis, differential scanning calorimetry, and water absorption studies was systematically studied.

2. Materials and methods

2.1. Materials

Polypropylene (PP) (grade name EL-Pro P702J) with density 0.91 g/cm^3, melting point 163 °C, and the melt flow index (230 °C, 2.16 kg) of 12 g/10 min was used as the starting material obtained from SCG plastics Co., Ltd, Thailand. Polylactic acid (PLA) (grade name Ingeo™ Biopolymer 3251D) with density 1.24 g/cm^3, melt flow rate 80 g/10 min (210 °C, 2.16 kg) and a melting point of 210 °C was supplied by NatureWorks, Minnetonka, United States. The cleaned sisal fiber (SF) was supplied by Hub Kaphong agricultural cooperatives, Phetchaburi, Thailand. The sisal fibers were cut into ca. 5 mm long and used as reinforcement for the composites.

2.2. Methods

2.2.1. Fabrication of composites

PP, PLA, and sisal fibers (SF) were dried overnight in an air oven at 80 °C before the preparation of the composites. PP and PLA based composites were extruded by co-rotating twin-screw extruders (XINDA SHJ-20, China) at 190 °C and 160 °C respectively, at a rotation speed of 100 rpm. The amount of sisal fibers content used was 10, 20 and 30 wt%. The composite extruded was cooled in a water-cooling bath and pelletized using a pelletizer Zhangjiagang Beisite Machinery, China. The samples were then dried in an air oven overnight at 80 °C. The dried samples were then injection molded using an ENGEL ES 200/50 – HL injection molding machine at 200 °C for PP composite and at 180 °C for PLA composite for the preparation of test specimens. The effect of recycling on the morphology, thermo-mechanical and water absorption was studied by repeating the procedure up to four times and the samples are referred to as R1, R2, R3, and R4. The composition and designation of the samples prepared are given in Table S1 (supplementary material).

3. Characterization

3.1. Mechanical properties

Universal testing machine (UTM) Comtech QC-601T, Taiwan was used to measure the tensile properties of the polymer composites according to ASTM D638 standards. The gauge length of 25 mm and a speed of 5 mm/min was used for testing the samples. At least five measurements of each sample were tested to determine the tensile properties.

3.2. Thermal characterization

Mettler Toledo TGA/DSC1, Switzerland was used to measure the thermal stability of the polymer composites. The weight of the samples used for testing was ca. 7 mg. The purge gas used was nitrogen with a flow rate of 40 ml/min. The test was conducted in a temperature range of 40–700 °C. The heating rate used was 10 K/min.

Mettler Toledo DSC/SDTA 821e, Switzerland was used to measure the melting and crystallization behaviors of the composites. The amount of the material used for DSC measurements was ca. 8 mg. The test was conducted from 30 to 200 °C with a heating rate of 10 K/min. The samples were then cooled to 30 °C at a rate of 10 K/min. The parameters such as melting temperature (T_m), cold

crystallization temperature (T_{cc}), enthalpy of melting (ΔH_m), enthalpy of crystallization (ΔH_c), enthalpy of cold crystallization (ΔH_{cc}) and degree of crystallinity (χ) of the polymer composites were determined as in our previous publications (Parameswaranpillai et al., 2019; Techawinyutham et al., 2019; Tengsuthiwat et al., 2019).

3.3. Scanning electron microscope (SEM)

Carl Zeiss ULTRA Plus scanning electron microscopes was used to investigate the morphology of the polymer composites. The SEM has been investigated on cryo-fractures. The samples were sputter coated with 1 nm thickness of gold using Q150R PLUS sputter coater (Quorum Technologies Ltd, UK).

3.4. Water absorption studies

Water absorption studies of the polymer composites were carried out according to ASTM D570-98 standard test method. The rectangular specimens ($19 \times 20 \times 3$ mm^3) were immersed in a distilled water for a period of 1560 h. The percentage weight gain at any time interval (M_t) was calculated using the Eq. (1). Where W_d is the initial weight of the composites and W_w *is* the weight of composites after exposure to water absorption.

$$Mt = \left(\frac{W_w - W_d}{W_d}\right) \times 100 \quad (1)$$

4. Result and discussion

4.1. Results of the repeated mechanical recycling process

During the successive recycling, high shear forces, temperature, and the presence of impurities in the polymer may induce polymer chain damage that may deteriorate the thermo-mechanical properties of the polymer composites. All the composites can be recycled well by injection molding except PLA/SF 80/20 and PLA/SF 70/30. The reprocessing after R2 caused problems during the demolding phase; the movement of ejector pins caused the formation of cracks that resulted in damaged samples. As a result, the repeated mechanical recycling process was stopped at R2 for PLA/SF 80/20 and PLA/SF 70/30 composites.

4.2. Tensile measurements

The effect of recycling on the mechanical properties of PP/sisal fiber composites and PLA/sisal fiber composites are shown in Fig. 1. The content of sisal fibers used for the modification of PP and PLA are 10, 20 and 30 wt%. From Fig. 1a, the tensile strength of the PP/sisal fiber composites (R0) shows fluctuations with the incorporation of sisal fibers. On the other hand, the tensile strength of the PP/sisal fiber composites marginally reduced with increasing recycling times from R0 to R4, maybe due to the dewetting effect (Favaro et al., 2010). The Young's modulus of PP is observed at

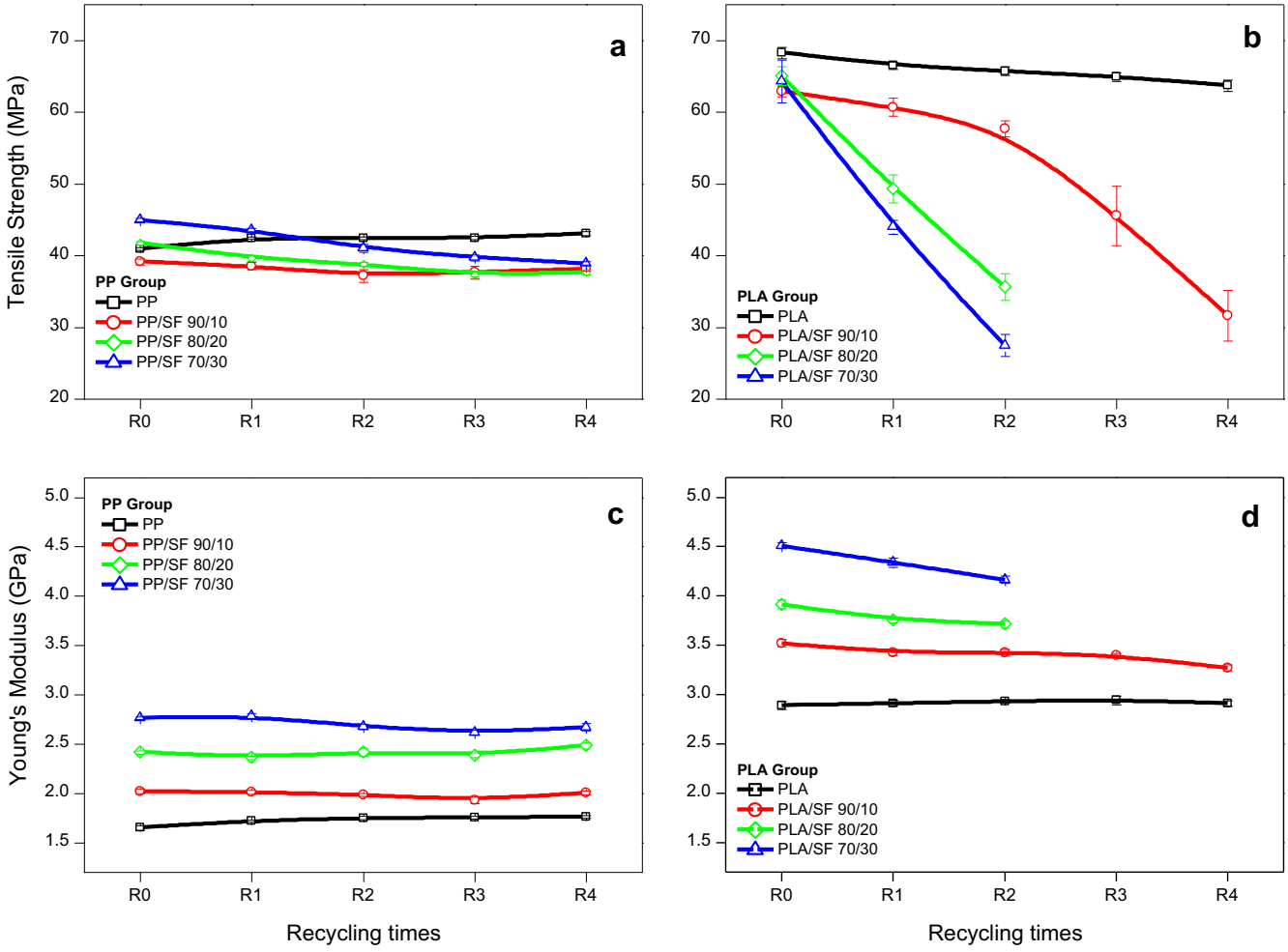

Fig. 1. The effect of recycling times on mechanical properties of sisal fiber composites with PP and PLA matrix (a–b, tensile strength), (c–d, Young's modulus).

1650 MPa and the modulus (Fig. 1c) increases dramatically with the addition of fibers and the maximum values of ca. 2760 MPa were recorded at 30 wt% fiber content. The increase in Young's modulus represents the enhancement in stiffness of the composites with the addition of fibers (Bourmaud and Baley, 2009; Bajpai et al., 2012). It is previously reported that Young's modulus of PP/sisal fiber composite decreases with recycling because of the reduction of the fiber aspect ratio (Bourmaud and Baley, 2007). Very recently Lila et al (2018) shown that the tensile strength and the modulus of the PP/bagasse fiber composites increase with recycling. The increase in mechanical properties is due to the increased aspect ratio of the fibers. The authors observed a reduction in length and diameter of the fibers (mechanical degradation of fibers) with recycling, however, the reduction in diameter is higher due to debundling of the fibers during the recycling process. In another interesting work, Bourmaud et al. (2011) reported that Young's modulus and tensile strength of recycled PP/hemp fiber composites remain stable due to the stability of the aspect ratio. Thus, the aspect ratio of the natural fibers is the key factor in determining the mechanical performance of the composites. In the case of PP/sisal composites, the tensile strength and Young's modulus are stable with respect to recycling times. That means the aspect ratio of the fibers is not varied much with repeated recycling. Additionally, PP is known for its exceptional recyclability and is an added advantage for making biocomposite (Bourmaud et al., 2011).

The variations in mechanical properties of the PLA composites with respect to recycling times are shown in Fig. 1b and d. It should be pointed out that the neat PLA shows a remarkably high tensile strength and modulus compared to neat PP matrix. The tensile strength is slightly reduced while the tensile modulus is increased with the incorporation of sisal fibers in the PLA matrix. However, the tensile strength drops dramatically, while Young's modulus drops marginally with successive recycling (from R0 to R4) and the drop is more prominent for the composites containing 20 and 30 wt% sisal fibers. In previous work, Pillin et al. (2008) have shown that the drop in molecular weight potentially decreases the mechanical properties of the PLA. Later Le Duigou et al. (2008) studied the mechanical properties of the PLLA/Flax fiber composites as a function of recycling. The authors observed a drop-in mechanical property due to fiber damage and polymer degradation. The fiber content plays a pivotal role in polymer degradation. This is because PLA is susceptible to hydrolytic degradation at high processing temperatures and the water content present in the fibers favor hydrolytic degradation of the PLA. Thus, fiber damage and chain scission of the polymer chains during recycling result in the drop in tensile strength and Young's modulus of the PLA composites.

4.3. Morphology of the polymer composites

Fig. 2 shows the SEM micrographs of neat PP and sisal fiber reinforced PP composites before and after recycling. The SEM images provide information on filler dispersion and filler-matrix adhesion (Srebrenkoska et al., 2008). Fig. 2a–c shows the SEM micrographs of the PP matrix of R0, R2, and R4. A single-phase morphology with

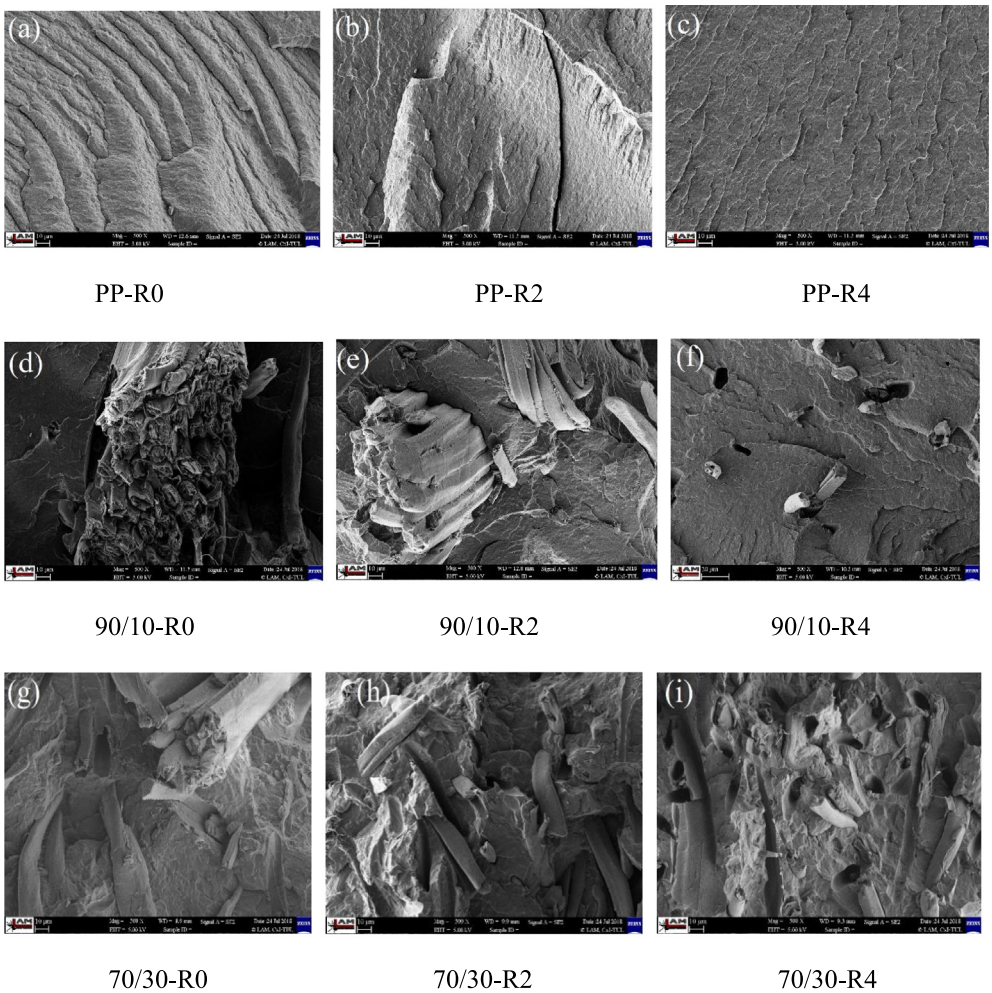

Fig. 2. SEM micrographs of neat PP and sisal fiber reinforced PP composites before and after recycling (a–c, neat group), (d–f, SF 10 wt%), (g–i, SF 30 wt%).

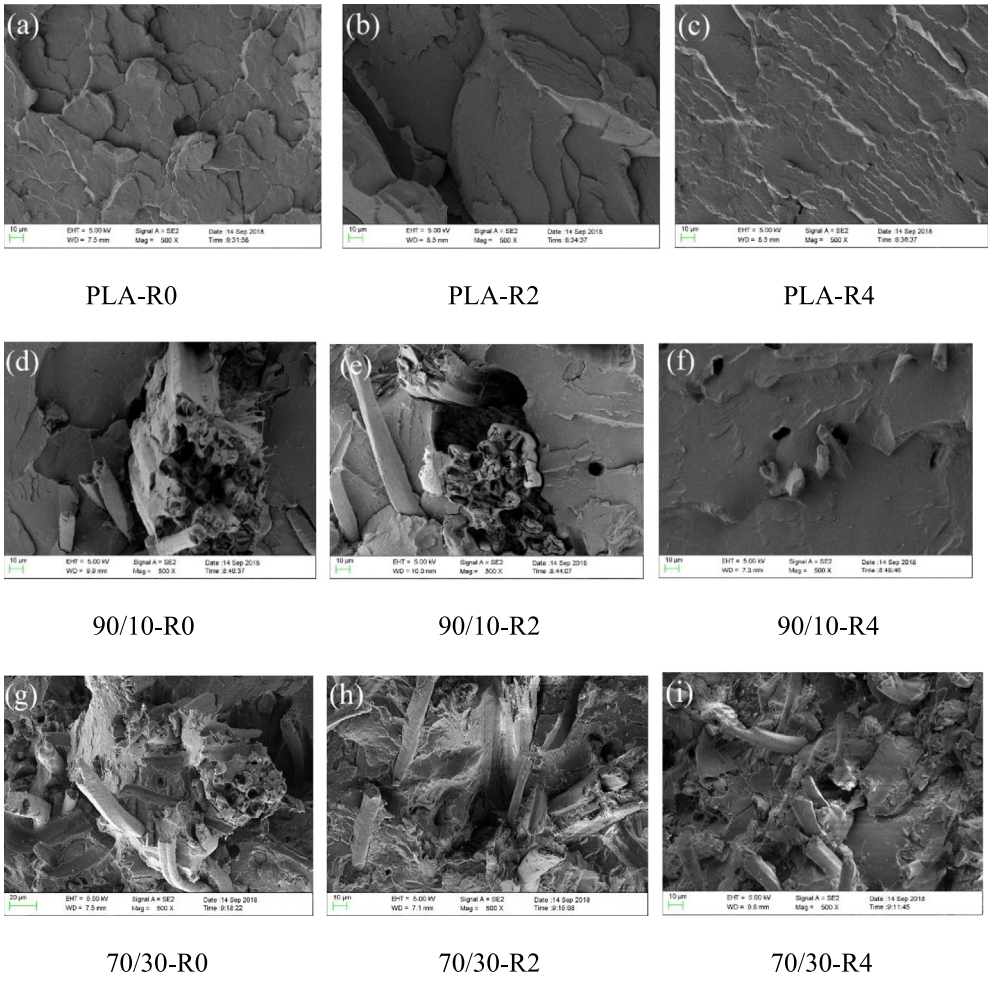

Fig. 3. SEM micrographs of neat PLA and sisal fiber reinforced PLA composites before and after recycling (a–c, neat group), (d–f, SF 10 wt%), (g–i, SF 30 wt%).

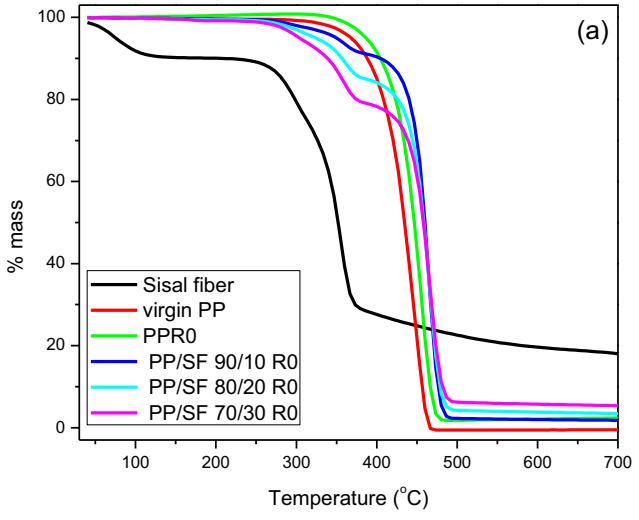

Fig. 4a. TGA thermogram of PP/SF composites as a function of SF contents at R0.

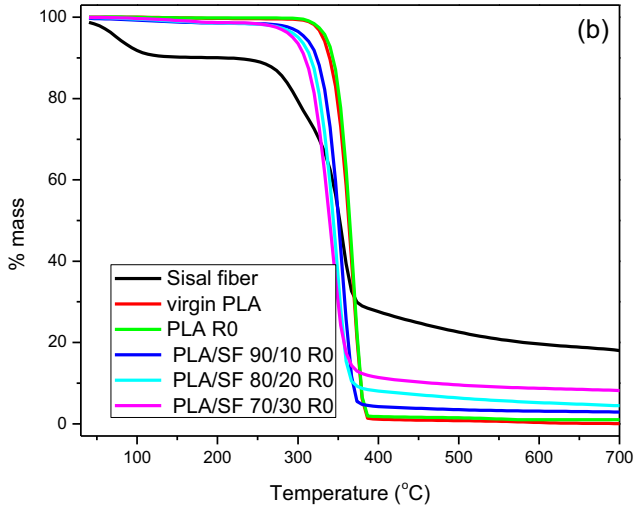

Fig. 4b. TGA thermogram of PLA/SF composites as a function of SF contents at R0.

ductile fractures is observed for the PP matrix. There is no significant change in the morphology of PP after R2 and R4 with respect to R0. Fig. 2d–f shows the SEM micrographs of PP/sisal composites having composition 90/10 after R0, R2, and R4. The sisal fibers are clearly observed in the PP matrix. Interestingly the fibers exist as bundles. Along with the fiber bundles, individual fibers are also observed throughout the matrix irrespective of the recycling and fiber content. The diameter of each fiber is ca. 10 μm. The fibers are pulled out of the matrix with the application of the applied load. Few micro-voids are observed at R4, which is an evidence

of the fiber debonding from the matrix indicating limited adhesion between the fiber and PP matrix. Therefore, the mechanical strength decreases with repeated recycling. This is concurrent with the results of Bourmaud and Baley (2007). The SEM micrographs of 70/30 composites are shown in Fig. 2g–i. From the micrographs of R4, few microvoids were observed in the PP matrix as in the case of 90/10 composites, these results revealed limited interfacial adhesion between the fibers and polymer matrix after successive recycling.

Fig. 3 shows the SEM micrographs of neat PLA and sisal fiber reinforced PLA composites containing 90/10 and 70/30 compositions before and after recycling (R0, R2, and R4). Single phase morphology with brittle fractures is observed for the PLA matrix (Fig. 3a–c). There are some significant changes in morphology after every recycling times. The fracture surface of the PLA matrix lost its identity in the R4, maybe due to the degradation of the PLA after repeated recycling (Beltrán et al., 2019). It should be pointed out that the tensile strength drops for the neat PLA after repeated recycling and these results are in line with SEM micrographs. Fig. 3d–f shows the SEM micrographs of PLA/sisal fiber composites having composition 90/10 after R0, R2 and R4 recycling times. Few micro-voids are observed at R2 and R4 recycling times due to limited interfacial adhesion between the fiber and the PLA matrix, also the matrix surface lost its behavior possibly due to the degradation of PLA matrix after a couple of recycling time. SEM micrographs of 70/30 sisal fiber modified PLA composites are shown in Fig. 3g–i. But it is unable to perform tensile measurements of 70/30 PLA/sisal composites after R2 due to the chain scission of the polymer samples resulting in shorter polymer chains that degrade at a lower temperature (Beltrán et al., 2019).

Table 1
T_i, T_f, and T_{max} of PP and PLA based composites.

Samples		T_i (°C)		T_f (°C)		T_{max} (°C)(Peak in the DTG curve)	
		Matrix type		Matrix type		Matrix type	
Sample groups	Recycling times	*PP*	*PLA*	*PP*	*PLA*	*PP*	*PLA*
PP and PLA	Neat	408.89	336.45	462.43	377.91	450.24	364.74
	R0	422.08	339.36	469.61	380.23	456.17	389.57
	R1	426.37	340.55	474.97	378.78	460.10	366.28
	R2	429.34	340.09	472.93	378.43	461.35	365.80
	R3	431.27	340.44	474.67	379.12	462.89	366.07
	R4	433.69	340.10	472.78	379.16	461.31	365.44
PP/SF and PLA/SF 90/10	R0	275.50	326.28	477.49	368.22	463.52	353.44
	R1	275.16	324.84	476.28	364.79	464.08	352.04
	R2	275.20	323.34	471.86	366.34	459.15	351.26
	R3	275.46	320.55	476.13	363.24	459.72	349.87
	R4	278.51	316.09	473.05	360.40	459.64	347.27
PP/SF and PLA/SF 80/20	R0	273.38	314.92	478.76	361.83	465.34	347.78
	R1	272.67	311.35	479.24	360.56	466.26	344.79
	R2	273.90	310.44	477.32	358.14	464.25	340.71
	R3	273.10	–	477.56	–	464.15	–
	R4	273.50	–	476.04	–	462.19	–
PP/SF and PLA/SF 70/30	R0	270.61	308.59	479.51	357.41	466.14	340.81
	R1	272.73	302.18	481.75	361.17	476.93	340.69
	R2	271.85	290.10	481.13	355.76	476.06	331.54
	R3	275.16	–	481.24	–	465.71	–
	R4	271.04	–	480.19	–	467.00	–
Sisal fiber	–	270.29		367.43		355.66	

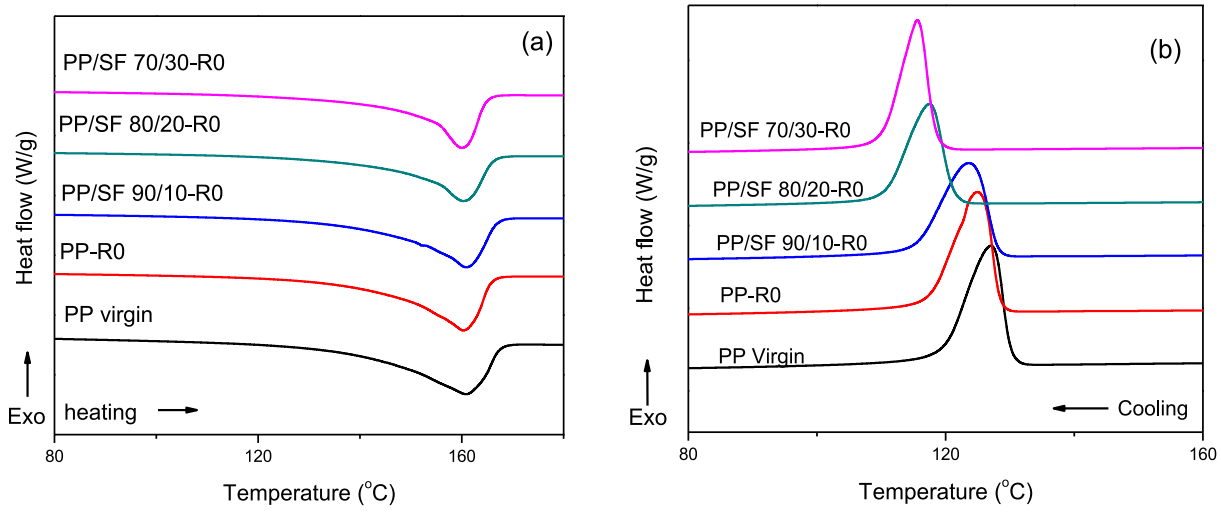

Fig. 5a and b. DSC (a) heating and (b) cooling curve of neat PP and PP/SF composites at R0.

4.4. Thermogravimetric analysis

Thermograms of PP/sisal fiber composites and PLA/sisal fiber composites are shown in Figs. 4a and 4b respectively. From Fig. 4a, the neat PP shows only a single degradation step in the thermogravimetric profile, but for composites, two degradation steps are observed. The first degradation at ca. 270 °C is due to the degradation of the fibers, while the second degradation at ca. 400 °C is due to the degradation of PP matrix. Two-step degradation is also observed for the recycled composites (Fig. S1 (supplementary materials)). The two-step degradation in the composites suggest the existence of fibers in the PP phase, that means the fibers are stable even after the repeated recycling. The char residue of the composites is slightly increased due to the high char content of the sisal fibers. On the other hand, PLA based composites (Fig. 4b) show only a single step degradation, this is because both fiber and PLA are degraded at almost the same temperature. The initial degradation temperature (T_i) is reduced for the PLA composites due to the presence of the sisal fibers. The shift in T_i to lower temperature suggests that the PLA degrade at a lower temperature. The initial degradation temperature (T_i), final degradation temperature (T_f), and maximum degradation temperature (T_{max}) of the composites studied are given in Table 1. Interestingly, successive recycling from R0 to R4 marginally enhances the T_i of neat PP (decomposition temperature of PP), while T_i of PP-based composites (decomposition temperature of natural fibers) remain stable. On the other hand, the recycling reduced T_i, T_{max}, and T_f, of the PLA based composites. Nevertheless, all the prepared composites are stable up to 250 °C.

4.4.1. Differential scanning calorimetry of PP-based composites

The melting and crystallization peaks of virgin PP, injection molded PP and sisal fiber modified PP composites are shown in Fig. 5a and b. From the heating curve, the melting temperature of PP is observed at ca. 160 °C, irrespective of the addition of fiber. On the other hand, from the cooling curve, the crystallization temperature (T_c) shift to lower temperature with the addition of fiber. With the increasing concentration of fibers, the T_c further shifted to a lower temperature. The shift in T_c to lower temperature point towards the lowering of crystallization rate of the PP matrix in the presence of fibers. This is because the fibers may hinder the

Table 2
The DSC parameters obtained for the PP-based composites at R0, R1, R2, R3, and R4.

Samples	T_m (°C)	ΔH_m (J/g)	T_c (°C)	ΔH_c (J/g)	X_c (%)
Virgin PP	161.67	88.62	124.67	96.24	42.79
PP-R0	160.35	88.79	125.02	93.18	42.87
PP-R1	160.27	90.90	125.18	91.75	43.89
PP-R2	160.21	97.14	125.48	93.57	46.9
PP-R3	160.84	99.32	125.33	95.96	47.96
PP-R4	161.03	96.76	125.32	101.26	46.72
90/10-R0	160.96	89.91	123.51	90.91	48.24
90/10-R1	160.78	91.51	123.53	92.65	49.1
90/10-R2	160.64	83.05	123.48	87.80	44.56
90/10-R3	160.47	80.46	123.13	89.35	43.17
90/10-R4	160.78	86.86	122.82	89.47	46.60
80/20-R0	160.28	69.46	117.45	75.63	41.92
80/20-R1	160.99	72.93	117.25	75.85	44.02
80/20-R2	160.33	67.24	116.29	75.79	40.58
80/20-R3	161.13	67.49	115.67	75	40.74
80/20-R4	159.96	72.34	115.54	75.22	43.66
70/30-R0	161.22	60.04	116.73	68.06	41.42
70/30-R1	160.83	61.50	115.95	66.94	42.42
70/30-R2	160.81	62.75	115.33	67.14	43.28
70/30-R3	160.52	57.11	115.07	65.53	39.39
70/30-R4	161.33	61.65	114.04	65.18	42.53

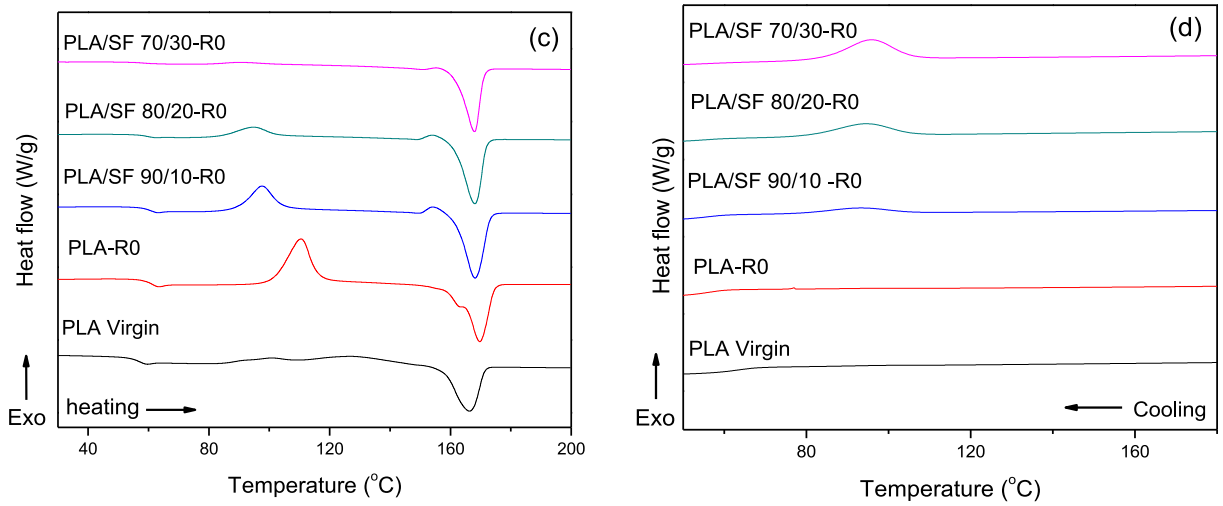

Fig. 5c and d. DSC thermographs of neat PLA and PLA based composites at R0.

polymer chains to migrate or diffuse towards the surface of the growing polymer crystal (Huda et al., 2008).

The variations in melting and crystallization thermogram of neat PP and its composites with different compositions at successive recycling times (R0, R1, R2, R3, and R4) are shown in Fig. S2 (supplementary material). The melting and crystallization temperature of PP and PP-based composites show an identical behavior irrespective of the successive recycling. The parameters obtained from the thermograms such as T_c, T_m, ΔH_m, and ΔH_c are given in Table 2. The percentage crystallinity of the PP matrix is calculated and the values obtained are also given in table 2. For neat PP and PP/sisal fiber composites, the T_m and T_c show only marginal variations with the successive recycling, that means the recycling has no effect or marginal effect on the polymer structure. Interestingly, the % crystallinity of the PP matrix increases with successive recycling. But for PP composites irrespective of the sisal fiber content, fluctuations in percentage crystallinity is observed with successive recycling. Studies have shown an increase in crystallinity of the polymers because of the higher chain mobility due to degradation (Le Duigou et al., 2008). Since recycling has no effect or marginal effect on the PP structure, the crystallinity did not change significantly.

4.4.2. Differential scanning calorimetry of PLA based composites

The melting and crystallization thermograms of neat PLA and sisal fiber reinforced PLA composites are shown in Fig. 5c and d. From the thermogram, the T_g values of the PLA composites are stable. However, a marginal drop in T_m for PLA composites is observed. A cold crystallization peak (T_{cc}) is observed for PLA-R0 at 100 °C, however, for the composites, the T_{cc} peak becomes broader and shifted to lower temperatures with increasing filler content and also the cold crystallization peak of PLA slowly disappear with increasing filler content. In fact, the cold crystallization peak completely disappears for 70/30-R0 composites. This implies that the sisal fibers acts as a nucleating agent their by importing the crystallization potential of the PLA matrix. Further, for PLA-R0, no *Tc* is observed this is because the crystallization rate is too slow. However, the T_c appears in the cooling curve for the composites. This results clearly imply that the fibers act as a heterogeneous nucleating agent for the crystallization of the composites thereby reducing the free energy barrier and improves the crystallization of the PLA matrix (Frone et al., 2013).

For the evaluation of the crystallization potential of the PLA composites. The % crystallinity was measured using the Eq. (2).

$$X = (\Delta H_m - \Delta H_{cc})/\Delta H_{max} \times W_{poly}) \times 100 \quad (2)$$

The values obtained are given in Table S2 (supplementary material). A remarkable increase in percentage crystallinity is observed for the PLA composites containing sisal fiber.

The DSC thermograms of neat PLA and its composites at different recycling times are shown in Fig. 6a–h. For neat PLA (Fig. 6a–b) a marginal decrease in T_m is observed with increasing recycling

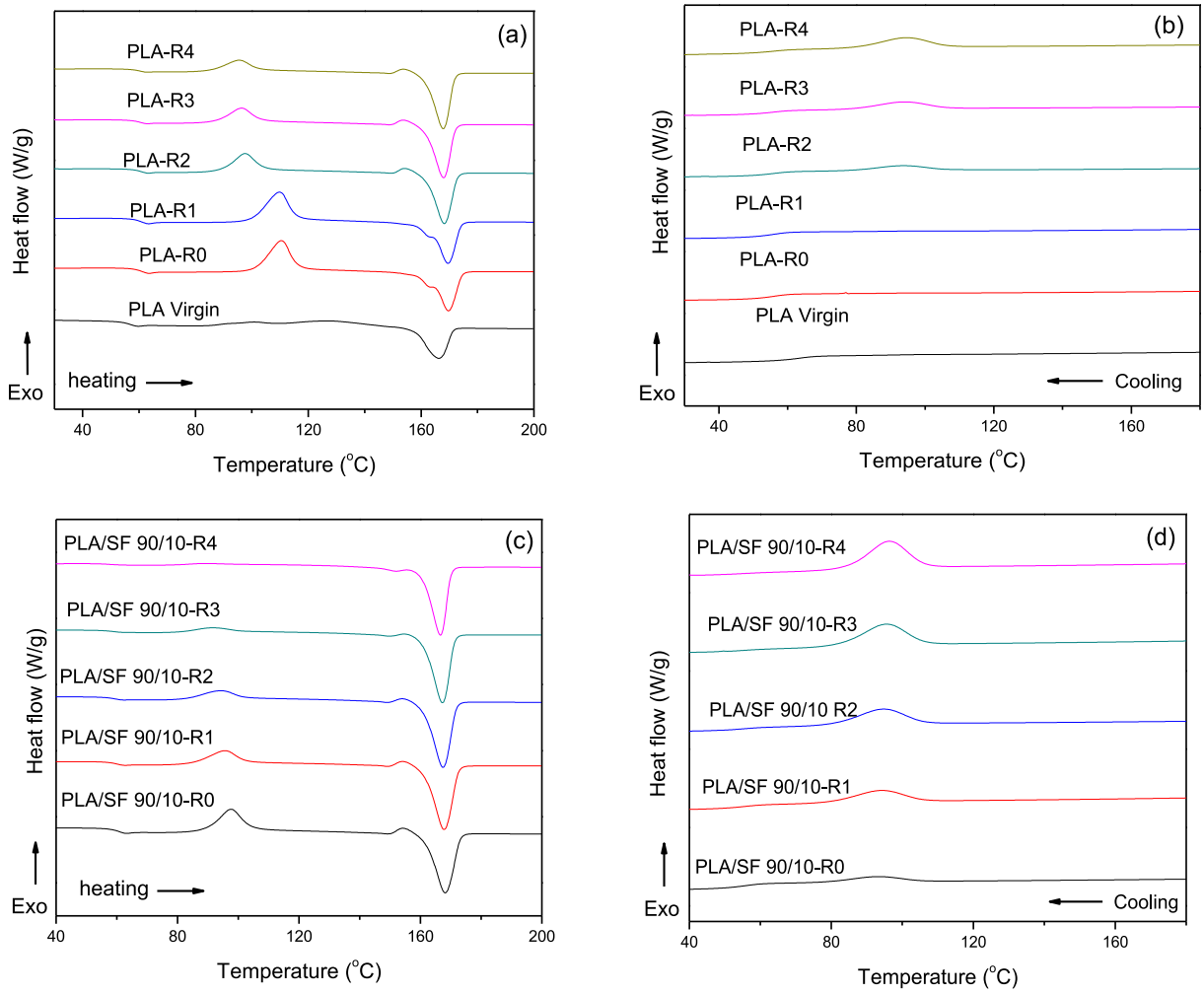

Fig. 6. DSC thermographs of neat PLA and PLA based composites at R0, R1, R2, R3, and R4.

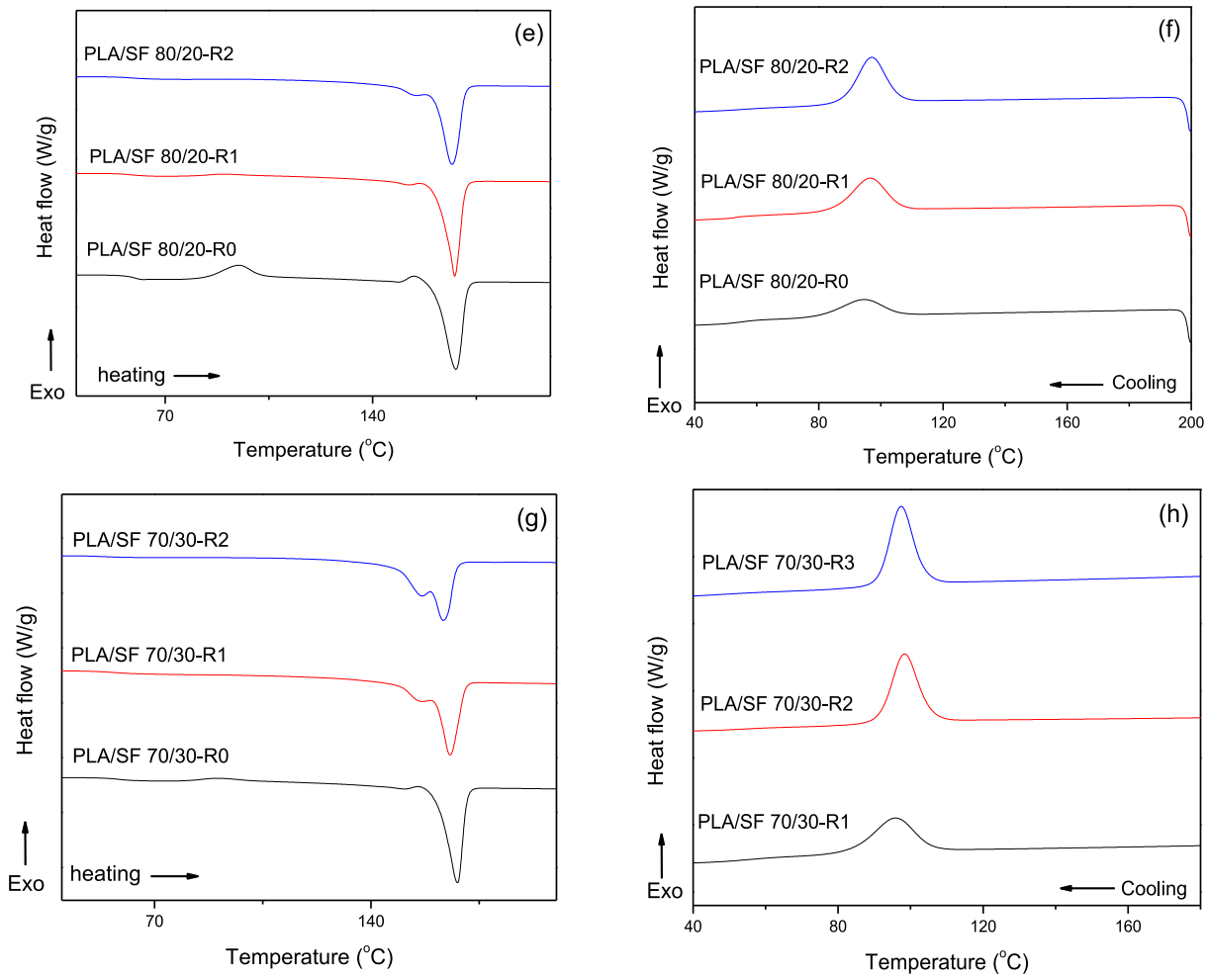

Fig. 6 (*continued*)

times. A sharp cooled crystallization peak is observed for neat PLA-R0 and PLA-R1 at 100 °C, however, T_{cc} slowly shifted to lower temperatures for PLA-R2, PLA-R3, and PLA–R4, and also the T_{cc} peak became less prominent at increasing recycling time. This is due to the increasing crystallization rate with repeated recycling times. On the other hand, there is no T_c in the cooling curves for neat PLA-R0 or PLA-R1, because the crystallization rate of PLA is too slow for PLA-R0 and PLA-R1. However, the T_c appeared in the cooling curve of PLA–R2, PLA–R3, and PLA–R4. This implies that the recycling process improves the crystallization rate of the neat PLA. This is due to the structural changes occurred during the recycling process.

Similar results are obtained for 90/10 PLA/sisal fiber reinforced composites (Fig. 6c–d) with T_c becomes more prominent while T_{cc} diminishes and shifted to lower temperature with increasing recycling times. For 80/20 PLA/sisal fiber composites (Fig. 6e–f), after the first recycling time, the T_{cc} is completely diminished, while the T_c becomes more prominent with no changes in T_m. For 70/30 PLA/sisal fiber composites (Fig. 6g–h), a small peak for T_{cc} is observed but it completely disappears with recycling from R0 to R2. On the other hand, the T_c become sharper at R1 and R2. Thus this study reveals that the fiber content and recycling acts synergistically to improve the crystallinity of the PLA based composites. The percentage crystallinity of all the composites studied is calculated using Eq. (2), and the obtained results are given in Table S2 (supplementary material). The results confirm that the PLA based composites show a substantial increase in crystallinity with both filler content and recycling. This is because the rate of crystallization increases with both fiber content and recycling. The increase in crystallinity may lead to shrinkage of the degraded samples leading to poor mechanical properties (Beg et al., 2007). Several authors cited the nucleating action of natural fibers on the polymer matrices (Wang and Liu, 1999; Zafeiropoulos et al., 2001). However, some studies have reported an increase in crystallinity because of the higher chain mobility due to degradation (Le Duigou et al., 2008). We assume that both these factors contribute to the crystallization of the PLA sisal fiber composites.

4.5. Water absorption studies

The water absorption behavior of PP and PLA based composites are shown in Fig. S3 (supplementary material). The water absorption is more for PLA based composites than PP, this is because PLA is more hydrophilic than PP. However, for both PP and PLA reinforced composites, the increasing sisal fiber content increases the water absorption, due to the hydrophilic nature of the sisal fibers. The water molecules form hydrogen bonding with the hydroxyl groups present in the cellulosic fibers and pave the way for the diffusion of water molecules into the matrix/fiber interface. Furthermore, the porous tubular structure of sisal fibers enables the diffusion of water molecules into the polymer composites through the capillary effect (Ashori and Sheshmani, 2010). In other words, as the fiber content increases the cellulosic content and the interfacial area between the fiber and polymer also increases and hence

more water diffuses into the composites (Alamri and Low, 2012). For PP-based composites, the water absorption decreases with increasing recycling times and is more pronounced in the case of 70/30 PP/SF composites. This may be due to better fiber distribution, improved fiber-matrix interface, increased hydrophobicity, lower void content, and shrinkage of the composites with repeated recycling (Tajvidi and Takemura, 2010). On the other hand, for PLA based composites the decrease in water absorption is not prominent after the first cycle. This is because the decrease in water absorption with recycling is eliminated with heating cycles and loops.

5. Conclusion

The PP and PLA based composites with sisal fibers were subjected to repeat recycling. The incorporation of sisal fibers has no significant effect on the tensile strength but enhanced Young's modulus of the composites. The fibers have a limited effect on the interfacial interaction between the fibers and matrix which explains the marginal changes in tensile properties of the composites. SEM micrographs revealed fiber pullout from the matrix. The PP matrix shows fluctuations in percentage crystallinity with the addition of fibers and with repeated recycling. On the other hand, the PLA matrix shows a remarkable increase in crystallinity by the addition of sisal fibers and with repeated recycling. The water absorption is increased with the addition of fibers but reduced with recycling times. In summary, it is viable to use agro-waste for developing polymer composites with excellent recyclability. More studies on the environmental assessment and the potential use of recycled natural fiber reinforced polymer composites for various applications are going on in our laboratory.

Acknowledgments

The authors are grateful to Natural Composites Research Group (NCR), Center of Innovation in Design and Engineering for Manufacturing (CoI-DEM) and Faculty of Mechanical Engineering of the Technical University of Liberec for laboratory support. This study was supported by the Erasmus+ Credit Mobility Program basis (KA107) and Specific University Research Grant by the Ministry of Education, Youth and Sports of the Czech Republic through the European Union - European Structural and Investment Funds in the frames of Operational Programme Research, Development and Education - project Hybrid Materials for Hierarchical Structures (HyHi, Reg. No. CZ.02.1.01/0.0/0.0/16_019/0000843).

Appendix A. Supplementary material

Supplementary data to this article can be found online at https://doi.org/10.1016/j.wasman.2019.07.038.

References

Abba, H.A., Nur, I.Z., Salit, S.M., 2013. Review of agro waste plastic composites production. J. Miner. Mater. Char. Eng. 1 (05), 271–279.
Abraham, E., Elbi, P.A., Deepa, B., Jyotishkumar, P., Pothen, L.A., Narine, S.S., Thomas, S., 2012. X-ray diffraction and biodegradation analysis of green composites of natural rubber/nanocellulose. Polym. Degrad. Stab. 97, 2378–2387.
Alamri, H., Low, I.M., 2012. Mechanical properties and water absorption behaviour of recycled cellulose fibre reinforced epoxy composites. Polym Test. 31 (5), 620–628.
Arzondo, L.M., Perez, C.J., Carella, J.M., 2005. Injection molding of long sisal fiber–reinforced polypropylene: effects of compatibilizer concentration and viscosity on fiber adhesion and thermal degradation. Polym. Eng. Sci. 45 (4), 613–621.
Ashori, A., Sheshmani, S., 2010. Hybrid composites made from recycled materials: moisture absorption and thickness swelling behavior. Bioresour. Technol. 101 (12), 4717–4720.
Bajpai, P.K., Singh, I., Madaan, J., 2012. Comparative studies of mechanical and morphological properties of polylactic acid and polypropylene based natural fiber composites. J. Reinf. Plast. Comp. 31 (24), 1712–1724.
Bourmaud, A., Baley, C., 2007. Investigations on the recycling of hemp and sisal fibre reinforced polypropylene composites. Polym. Degrad. Stab. 92, 1034–1045.
Bourmaud, A., Baley, C., 2009. Rigidity analysis of polypropylene/vegetal fibre composites after recycling. Polym. Degrad. Stab. 94 (3), 297–305.
Bourmaud, A., Le Duigou, A., Baley, C., 2011. What is the technical and environmental interest in reusing a recycled polypropylene–hemp fibre composite? Polym. Degrad. Stab. 96 (10), 1732–1739.
Beltrán, F.R., Infante, C., de la Orden, M.U., Urreaga, J.M., 2019. Mechanical recycling of poly (lactic acid): evaluation of a chain extender and a peroxide as additives for upgrading the recycled plastic. J. Clean. Prod. 219, 46–56.
Beg, M.D.H., 2007. The Improvement of Interfacial Bonding, Weathering, and Recycling of Wood Fibre Reinforced Polypropylene Composites Ph.D. Thesis. The University of, Waikato, Hamilton, New Zealand, March.
Cestari, S.P., da Silva Freitas, D.D.F., Rodrigues, D.C., Mendes, L.C., 2019. Recycling processes and issues in natural fiber-reinforced polymer composites. In: Green Composites for Automotive Applications. Woodhead Publishing, pp. 285–299.
Chen, W.T., Jin, K., Linda Wang, N.H., 2019. Use of supercritical water for the liquefaction of polypropylene into oil. ACS Sustain. Chem. Eng. 7 (4), 3749–3758.
Chianelli-Junior, R., Reis, J.M.L.D., Cardoso, J.L., Castro, P.F., 2013. Mechanical characterization of sisal fiber-reinforced recycled HDPE composites. Mat. Res. 16 (6), 1393–1397.
Cicala, G., Pergolizzi, E., Piscopo, F., Carbone, D., Recca, G., 2018. Hybrid composites manufactured by resin infusion with a fully recyclable bioepoxy resin. Compos. Part B Eng. 132, 69–76.
Cicala, G., Tosto, C., Latteri, A., La Rosa, A.D., Blanco, I., Elsabbagh, A., Russo, P., Ziegmann, G., 2017. Green composites based on blends of polypropylene with liquid wood reinforced with hemp fibers: thermomechanical properties and the effect of recycling cycles. Materials 10 (9), 998.
Dairi, B., Djidjelli, H., Boukerrou, A., Migneault, S., Koubaa, A., 2017. Morphological, mechanical, and physical properties of composites made with wood flour-reinforced polypropylene/recycled poly (ethylene terephthalate) blends. Polym. Compos. 38 (8), 1749–1755.
Das, K., Adhikary, K., Ray, D., Bandyopadhyay, N.R., 2010. Development of recycled polypropylene matrix composites reinforced with waste jute caddies. J. Reinf. Plast. Comp. 29 (2), 201–208.
Elsawy, M.A., Kim, K.H., Park, J.W., Deep, A., 2017. Hydrolytic degradation of polylactic acid (PLA) and its composites. Renew. Sust. Energ. Rev. 79, 1346–1352.
Geyer, R., Jambeck, J.R., Law, K.L., 2017. Production, use, and fate of all plastics ever made. Sci. Adv. 3 (7), e1700782.
Favaro, S.L., Ganzerli, T.A., de Carvalho Neto, A.G.V., Da Silva, O.R.R.F., Radovanovic, E., 2010. Chemical, morphological and mechanical analysis of sisal fiber-reinforced recycled high-density polyethylene composites. Express Polym. Lett. 4 (8), 465–473.
Frone, A.N., Berlioz, S., Chailan, J.F., Panaitescu, D.M., 2013. Morphology and thermal properties of PLA–cellulose nanofibers composites. Carbohyd. Polym. 91 (1), 377–384.
Gu, L., Ozbakkaloglu, T., 2016. Use of recycled plastics in concrete: a critical review. Waste Manage. 51, 19–42.
Huda, M.S., Drzal, L.T., Ray, D., Mohanty, A.K., Mishra, M., 2008. Natural-fiber composites in the automotive sector. In: Properties and Performance of Natural-fibre Composites. Woodhead Publishing, pp. 221–268.
Ibrahim, I.D., Jamiru, T., Sadiku, R.E., Kupolati, W.K., Agwuncha, S.C., 2017. Dependency of the mechanical properties of sisal fiber reinforced recycled polypropylene composites on fiber surface treatment, fiber content and nanoclay. J. Polym. Environ. 25 (2), 427–434.
Laadila, M.A., Hegde, K., Rouissi, T., Brar, S.K., Galvez, R., Sorelli, L., Abokitse, K., 2017. Green synthesis of novel biocomposites from treated cellulosic fibers and recycled bio-plastic polylactic acid. J. Clean. Prod. 164, 575–586.
Lila, M.K., Singhal, A., Banwait, S.S., Singh, I., 2018. A recyclability study of bagasse fiber reinforced polypropylene composites. Polym. Degrad. Stab. 152, 272–279.
Le Duigou, A., Pillin, I., Bourmaud, A., Davies, P., Baley, C., 2008. Effect of recycling on mechanical behaviour of biocompostable flax/poly (l-lactide) composites. Compos. Part A Appl. Sci. Manuf. 39 (9), 1471–1478.
Najafi, S.K., 2013. Use of recycled plastics in wood plastic composites – a review. Waste Manage. 33 (9), 1898–1905.
Parameswaranpillai, J., Pulikkalparambil, H., Sanjay, M.R., Siengchin, S., 2019. Polypropylene/high-density polyethylene-based blends and nanocomposites with improved toughness. Mater. Res. Express 6, 075334.
Pillin, I., Montrelay, N., Bourmaud, A., Grohens, Y., 2008. Effect of thermo-mechanical cycles on the physico-chemical properties of poly (lactic acid). Polym. Degrad. Stab. 93 (2), 321–328.
Quynh Truong Hoang, T., Lagattu, F., Brillaud, J., 2010. Natural fiber-reinforced recycled polypropylene: microstructural and mechanical properties. J. Reinf. Plast. Comp. 29 (2), 209–217.
Singh, N., Hui, D., Singh, R., Ahuja, I.P.S., Feo, L., Fraternali, F., 2017. Recycling of plastic solid waste: a state of art review and future applications. Compos. Part B Eng. 115, 409–422.

Sanjay, M.R., Madhu, P., Jawaid, M., Senthamaraikannan, P., Senthil, S., Pradeep, S., 2018. Characterization and properties of natural fiber polymer composites: a comprehensive review. J. Clean. Prod. 172, 566–581.

Senthilkumar, K., Saba, N., Rajini, N., Chandrasekar, M., Jawaid, M., Siengchin, S., Alotman, O.Y., 2018. Mechanical properties evaluation of sisal fibre reinforced polymer composites: a review. Constr. Build. Mater. 174, 713–729.

Sanjay, M.R., Siengchin, S., Parameswaranpillai, J., Jawaid, M., Pruncu, C.I., Khan, A., 2019. A comprehensive review of techniques for natural fibers as reinforcement in composites: preparation, processing and characterization. Carbohyd. Polym. 207, 108–121.

Srebrenkoska, V., Gaceva, G.B., Avella, M., Errico, M.E., Gentile, G., 2008. Recycling of polypropylene-based eco-composites. Polym. Int. 57, 1252–1257.

Srivabut, C., Ratanawilai, T., Hiziroglu, S., 2018. Effect of nanoclay, talcum, and calcium carbonate as filler on properties of composites manufactured from recycled polypropylene and rubberwood fiber. Constr. Build. Mater. 162, 450–458.

Tajvidi, M., Takemura, A., 2010. Recycled natural fiber polypropylene composites: water absorption/desorption kinetics and dimensional stability. J. Polym. Environ. 18 (4), 500–509.

Techawinyutham, L., Siengchin, S., Parameswaranpillai, J., Dangtungee, R., 2019. Antibacterial and thermo-mechanical properties of composites of polylactic acid (PLA) modified with capsicum oleoresin (CO) impregnated nanoporous silica. J. Appl. Polym. Sci. 2019 (136), 47825.

Tengsuthiwat, J., Yorseng, K., Siengchin, S., Parameswaranpillai, J., 2019. Thermomechanical, water absorption, ultraviolet resistance and laser-assisted electroless plating behavior of Cu2O and melamine–formaldehyde-coated sisal fiber-modified poly (lactic acid) composites. Polym. Compos. https://doi.org/10.1002/pc.25182.

Thomas, M.G., Abraham, E., Jyotishkumar, P., Maria, H.J., Pothen, L.A., Thomas, S., 2015. Nanocelluloses from jute fibers and their nanocomposites with natural rubber: preparation and characterization. Int. J. Biol. Macromol. 81, 768–777.

Wang, C., Liu, C.R., 1999. Transcrystallization of polypropylene composites: nucleating ability of fibres. Polymer 40 (2), 289–298.

Zafeiropoulos, N.E., Baillie, C.A., Matthews, F.L., 2001. A study of transcrystallinity and its effect on the interface in flax fibre reinforced composite materials. Compos. Part A Appl. Sci. Manuf. 32 (3–4), 525–543.